

Multimodal Fact Checking with Unified Visual, Textual, and Contextual Representations

Aditya Kishore, Gaurav Kumar, Jasabanta Patro

Department of Data Science and Engineering
Indian Institute of Science Education and Research, Bhopal, India
{adityak21, gaurav22, jpatro}@iiserb.ac.in

Abstract—The growing rate of multimodal misinformation, where claims are supported by both text and images poses significant challenges to fact-checking systems that rely primarily on textual evidence. In this work, we propose a unified framework for fine-grained multimodal fact verification called MultiCheck, designed to reason over structured textual and visual signals. Our architecture combines dedicated encoders for text and images with a fusion module that captures cross-modal relationships using element-wise interactions. A classification head then predicts the veracity of a claim, supported by a contrastive learning objective that encourages semantic alignment between claim-evidence pairs in a shared latent space. We evaluate our approach on the Factify 2 dataset, achieving a weighted F1 score of 0.84, substantially outperforming the baseline. These results highlight the effectiveness of explicit multimodal reasoning and demonstrate the potential of our approach for scalable and interpretable fact-checking in complex, real-world scenarios.

I. INTRODUCTION:

Misinformation has become a serious concern in today's digital environment, affecting many areas like politics, public health, and finance [1]. While early instances of false information were mostly text-based [2], [3], [4], modern misinformation campaigns increasingly blend text with images, audio, and video making them more persuasive and harder to detect [5], [6], [7]. This rise in multimodal misinformation reveals the limitations of traditional fact-checking systems, which primarily focus on textual content [8], [9], [6]. In response, the research community has turned to multimodal fact-checking, where claims are verified using both textual and visual contents [10], [9]. Recent benchmarks such as FEVER [11], Mocheg [12], and Factify 2 [13] have helped advance research in this direction, see section II for further details. Multimodal fact-checking remains a difficult and open challenge. This is because, the task goes beyond simple classification. It requires understanding how modalities interact and whether they support or contradict each other. For example in Figure 1, where a claim is paired with a scientific image that appears credible but is actually unrelated. Identifying this mis-

match requires more than surface-level alignment. Thus we need a structured reasoning across both textual and visual modalities.

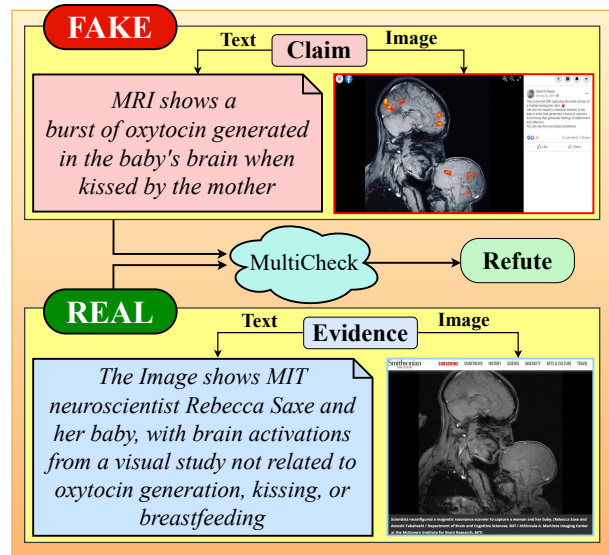


Fig. 1: Refuting a viral claim using combined text and image evidence.

Existing methods relied on one of two strategies: (i) concatenating image-text embeddings [14], [15], or (ii) joining vision and language encoders through late fusion [16]. For example, MOCHEG[12] processes claims and evidence through modality-specific encoders and fuses their outputs without deep cross-modal interaction, whereas PRO-COFACTV2[17] leverages attention-based mechanisms. While these strategies capture basic correlations, they often fail to detect fine contradictions or poorly aligned semantics. We believe they fail to separate modality-specific support signals and make the reasoning process transparent. We, on the other hand, have proposed a unified fact-checking framework called "MultiCheck", where we used (i) a novel **fusion technique**, which captures semantic relation via element-wise difference and product operations, and (ii) a **contrastive learning objective** that aligns semantically similar claim-document

pairs in a shared latent space, improving representation consistency across modalities. Our approach is inspired by prior advances in multimodal relational reasoning. The element-wise difference and product were shown to be capturing fine-grained interactions between paired inputs in natural language inference models [18] and bilinear attention models [19]. These operations encode both alignment and divergence between two modalities, enabling more expressive cross-modal representations. To further strengthen semantic alignment, we integrated a contrastive head that serves the objective of contrastive learning that operates on projected claim-document embeddings. This module is trained with a symmetric InfoNCE loss [20], encouraging the model to align semantically related pairs while pushing apart unrelated ones. Unlike prior methods that used frozen embeddings or shallow probes [21], our model is fully trainable end-to-end and jointly optimizes for both classification and contrastive learning, resulting in a more discriminative and robust representation for multimodal fact verification.

Our contributions are as follows:

- We have introduced a unified multimodal fact-checking architecture, "**MultiCheck**", that combines structured text and image features. It incorporates a **contrastive head** and a **fusion module** to align semantically related claim-evidence pairs while separating unrelated ones. As a result, we achieved a new state-of-the-art with the weighted F1 score of **0.84**, outperforming the baseline by **27%**.
- We have conducted thorough ablations to assess the impact of different backbones, fusion strategies, and training objectives. The results reveal that relational fusion using difference and product consistently outperforms simple concatenation, and that the inclusion of the contrastive loss significantly boosts performance, particularly in ambiguous or weak evidence scenarios.
- We have performed a comprehensive error analysis using statistical significance tests, showing that our model not only outperforms the baseline but does so in a structurally meaningful way, correcting more errors than it introduces. Discordant pair comparisons and contingency heatmaps analyses reveals consistent improvements across challenging veracity classes.
- We further supported our findings through qualitative analysis, highlighting how OCR cues and visual metadata can decisively shift predictions in subtle cases often missed by prior systems.

II. RELATED WORK

Recent research in automated fact-checking has highlighted the growing importance of incorporating multiple

modalities, to tackle the diverse and evolving forms of misinformation [22]. Early works, such as FEVER [23] and CLEF2018 [24] are primarily focused on verifying textual claims, laying foundational methods for claim verification based solely on textual evidence. However, later studies found that misinformation exploits images, videos, and audio alongside text to build convincing narratives [25], [26]. These studies have revealed the limitations of purely text-based fact-checking methods and sparked a shift toward multimodal fact-checking. To tackle the limitation of text-based methods, systems were designed to jointly process and reason over diverse types of content. For example, several studies, such as [16] and [27], [28], have explored architectures that integrated textual and visual features. These models employ mechanisms like attention or contrastive learning to enhance detection accuracy. Recent work by [29] shows that a probing classifier combining separate text and image embeddings can outperform intrinsic VLM features on datasets like Factify 2. In addition to these developments, comprehensive surveys, such as [10], offers detailed overview regarding the emerging field of multimodal fact-checking. They highlighted both the technical challenges and the promising research directions ahead. Key challenges include aligning information across modalities, managing incomplete or noisy evidence, and ensuring scalability for practical deployment.

Despite significant progress, effectively integrating multimodal information remains an open research problem. This challenge continues to motivate the development of new architectures and learning methods. Robust fact verification in multimodal contexts still requires innovative solutions.

III. DATASET DETAILS:

We have used the Factify-2 dataset [30] in our experiments. It is a large-scale multimodal dataset with 50,000 annotated claims spanning across domains such as politics, health, and global affairs. Claims were collected from verified news accounts on Twitter and trusted fact-checking platforms such as PolitiFact¹, Alt News², and BoomLive³. Each sample includes a claim-evidence pair with separate text, image, and OCR text, as shown in Figure 2. Unlike prior datasets such as Weibo [31], FakeNewsNet [32], and Mocheq [33], Factify-2 provides both text and image modalities at the claim level, enabling fine-grained multimodal verification. Claims are labeled one of the five labels based on their relationship with the evidence. Since the original test set was not publically available, we followed split protocol of prior work [29],

¹<https://www.politifact.com>

²<https://www.altnews.in>

³<https://www.boomlive.in>

by using the original validation set for testing and reallocating 7,500 training samples for validation. Table I shows the class distributions.

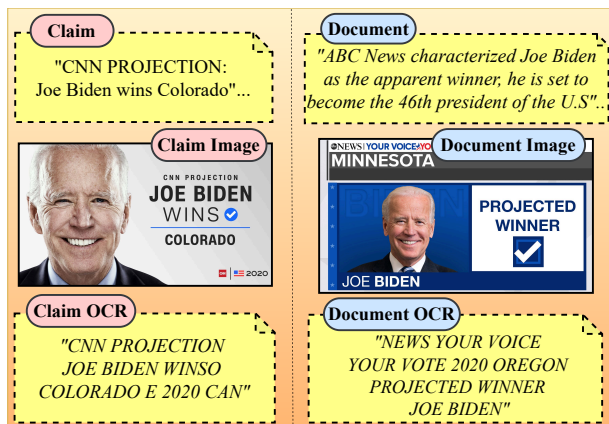


Fig. 2: Example of a sample from the dataset.

Factify 2 [30]				
Classes	Train	Validation	Test	Total
Support_Multimodal	5,580	1,420	1,500	8,500
Support_Text	5,485	1,515	1,500	8,500
Insufficient_Multimodal	5,472	1,528	1,500	8,500
Insufficient_Text	5,494	1,506	1,500	8,500
Refute	5,469	1,531	1,500	8,500
Total	27,500	7,500	7,500	42,500

TABLE I: Dataset statistics for Factify 2 across training, validation, and test splits.

IV. METHODOLOGY

In this section, we have reported our proposed framework, schematically depicted in Figure 4. Our framework has four components, i.e. (i) text module, (ii) image module, (iii) fusion module, and (iv) classification module. Each component of our framework is described as follows,

Text module: This module converts the claims, associated evidence documents and OCR texts extracted from images into an embedding space. For each instance, we concatenate the claim text with the OCR text from associated images to build a richer, context-aware representation. This fused input helps capture nuances that may not be evident in the claim alone. For example, in Figure 3, the OCR content reveals contradicting cues absent from the main claim, enabling more accurate veracity detection. We have used pre-trained language models such as RoBERTa [34], DeBERTa [35], or SBERT [36] for this purpose. This yields token IDs and attention masks of shape $\mathbb{R}^{b \times L}$, where b is the batch size and L is the sequence length. Each sequence is processed through a shared encoder to produce contextual embeddings:

$$\mathbf{H}_{\text{text}} \in \mathbb{R}^{b \times L \times d_{\text{text}}}$$

Here, d_{text} is the hidden size of the language model (e.g., 1024 for RoBERTa and DeBERTa, 768 for SBERT). We extract the [CLS] token embedding as a compact sequence representation: $\mathbf{h}_{[\text{CLS}]} \in \mathbb{R}^{b \times d_{\text{text}}}$

To align this with other modalities, we have projected the [CLS] embedding into a shared latent space using a linear transformation:

$$\mathbf{V}_{\text{text}} = \mathbf{W}_{\text{text}} \cdot \mathbf{h}_{[\text{CLS}]} + \mathbf{B}, \quad \mathbf{V}_{\text{text}} \in \mathbb{R}^{b \times h}$$

Here, h denotes the latent dimension, \mathbf{W}_{text} is the projection weight matrix, and \mathbf{B} is a bias term.

This module ensures that semantic and contextual information from both textual and OCR channels is preserved and embedded into a format suitable for cross-modal fusion in downstream stages.

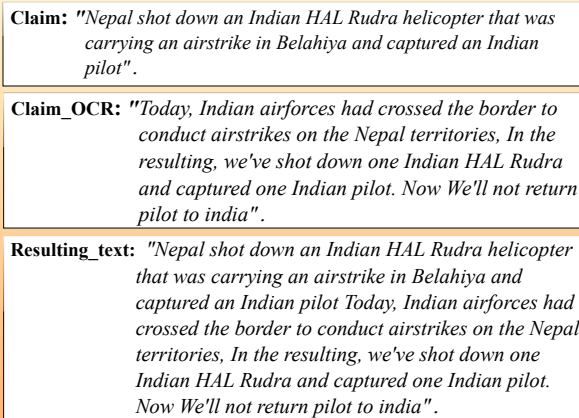


Fig. 3: Illustration: The claim suggests Nepal shot down an Indian helicopter. However, the OCR text contradicts this by suggesting Indian aggression, not Nepali. Without OCR, the model could misclassify this. The fused text representation enables correct "Refute" labeling.

Image module: The image module encodes the visual evidence associated with claims and supporting evidence documents into a shared embedding space. Each image is first preprocessed and passed through a shared vision encoder either ResNet50 [37] or Vision Transformer (ViT) [38]. This produces visual features of shape $\mathbf{f}_{\text{img}} \in \mathbb{R}^{b \times d_{\text{img}}}$, where b is the batch size and d_{img} corresponds to the raw output dimension (2048 for ResNet and 768 for ViT). To align with the text representation space, we project these features into a shared latent space using a linear transformation:

$$\mathbf{V}_{\text{img}} = \mathbf{W}_{\text{img}} \cdot \mathbf{f}_{\text{img}} + \mathbf{B}, \quad \mathbf{V}_{\text{img}} \in \mathbb{R}^{b \times h}$$

Here, \mathbf{W}_{img} is the projection matrix, \mathbf{B} is the bias term, and h denotes the shared latent dimensionality. To ensure compatibility for multimodal reasoning, both text and image embeddings are projected into the same vector space through modality-specific linear layers. At the end of this module, we obtain four representative

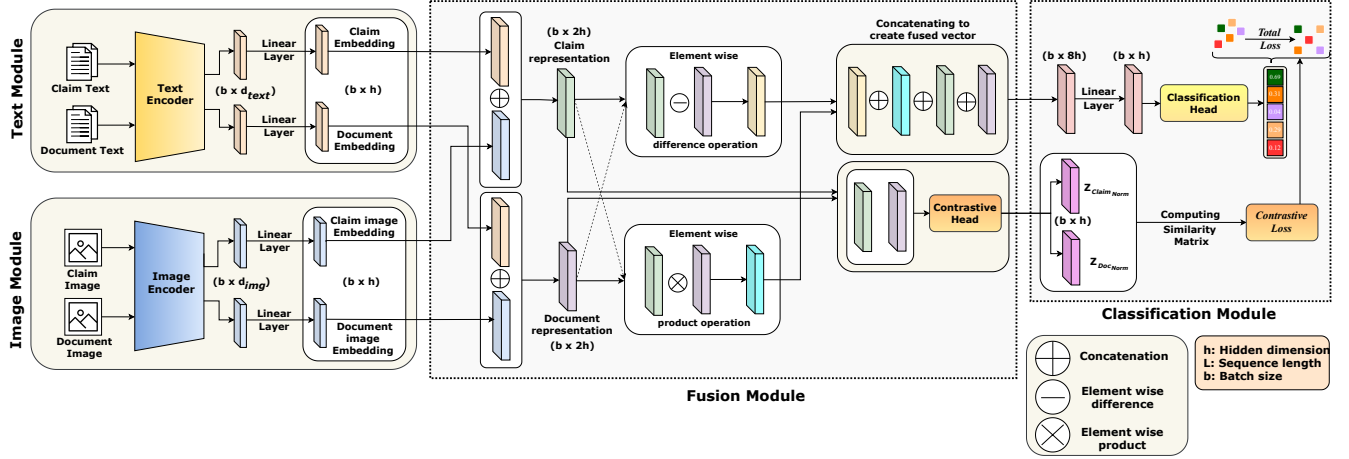


Fig. 4: Intuitive fusion representation using element-wise difference and product.

vectors of shape $\mathbb{R}^{b \times h}$: $\mathbf{V}_{\text{claim text}}$ and $\mathbf{V}_{\text{doc text}}$ from the text module, and $\mathbf{V}_{\text{claim img}}$ and $\mathbf{V}_{\text{doc img}}$ from the image module. These embeddings serve as the inputs for the fusion and classification modules that follow.

Fusion module: Our key innovation lies in the fusion module. It is designed to capture both direct and relational interactions between multimodal evidence. Prior systems rely on simple feature concatenation [39], [40], [41]. In contrast, our framework explicitly captures alignment and divergence between claim and document evidence. It uses element-wise difference and product operations over their multimodal representations embeddings. This approach is inspired by relational reasoning techniques shown effective in prior research [19], [18], [14], [42], [43].

Specifically, We first generated two integrated multimodal representations by concatenating text and image embeddings for the claim and the document:

$$\begin{aligned}\mathbf{V}_{\text{claim repr}} &= \mathbf{V}_{\text{claim text}} \oplus \mathbf{V}_{\text{claim img}} \\ \mathbf{V}_{\text{doc repr}} &= \mathbf{V}_{\text{doc text}} \oplus \mathbf{V}_{\text{doc img}}\end{aligned}$$

To extract finer relationships, we then computed (i) *element-wise difference*: which highlights differences between claim and document representations, and (ii) *element-wise product*: which emphasizes regions of strong alignment, between those two vectors denoted by:

$$\begin{aligned}\mathbf{V}_{\text{diff}} &= |\mathbf{V}_{\text{claim repr}} \ominus \mathbf{V}_{\text{doc repr}}| \\ \mathbf{V}_{\text{prod}} &= \mathbf{V}_{\text{claim repr}} \otimes \mathbf{V}_{\text{doc repr}}\end{aligned}$$

where \ominus and \otimes denote element-wise difference and product, respectively. It helps in determining, whether the multimodal input supports, refutes, or fails to verify a claim. Finally, these four vector embeddings: the claim representation, evidence document representation, difference, and product are concatenated, denoted by:

$$\mathbf{V}_{\text{fused}} = \mathbf{V}_{\text{diff}} \oplus \mathbf{V}_{\text{prod}} \oplus \mathbf{V}_{\text{claim repr}} \oplus \mathbf{V}_{\text{doc repr}}$$

Where \oplus shows the operation of concatenation. The fused vector is passed through a feedforward network with GELU activation [44], and dropout, yielding the final fused vector used for classification, denoted by:

$$\mathbf{V}_{\text{final}} = \text{FFN}(\mathbf{V}_{\text{fused}}) \in \mathbb{R}^{b \times h}$$

Where h denotes the dimensionality of the shared latent space and b shows the batch-size. This final fused representation captures refined multimodal interactions critical for reliable fact verification. To complement the supervised classification objective, we have incorporated a contrastive projection head that encourages semantic alignment between matching claim-document pairs. Each multimodal representation is passed through a shared two-layer projection network:

$$\begin{aligned}\mathbf{Z}_{\text{claim}} &= f_{\text{proj}}(\mathbf{V}_{\text{claim repr}}) \\ \mathbf{Z}_{\text{doc}} &= f_{\text{proj}}(\mathbf{V}_{\text{doc repr}})\end{aligned}$$

where the projection function f_{proj} is defined as:

$$f_{\text{proj}}(\mathbf{v}) = \mathbf{W}_2 \cdot \text{ReLU}(\mathbf{W}_1 \cdot \mathbf{v} + \mathbf{B}_1) + \mathbf{B}_2$$

where \mathbf{v} is the concatenated multimodal representation of either claim or the evidence document, $\mathbf{W}_1 \in \mathbb{R}^{h \times 2h}$ and $\mathbf{W}_2 \in \mathbb{R}^{h \times h}$, and $\mathbf{B}_1, \mathbf{B}_2$ are bias terms. This bottleneck structure reduces the concatenated vector from $2h$ to h and reprojects it, enabling richer discriminative representations. The resulting embeddings, $\mathbf{Z}_{\text{claim}}$ and \mathbf{Z}_{doc} , are used during training to compute a symmetric InfoNCE loss [20]. This loss encourages the model to pull together representations of matching claim-document pairs while pushing apart those of unrelated ones. By aligning semantically similar inputs across modalities, the contrastive learning objective improves the model's sensitivity to subtle semantic differences across modalities and strengthens its generalization capabilities.

Classification module: The classification module translates the fused multimodal representation into a final

prediction over five fine-grained veracity classes. The final fused vector $\mathbf{V}_{\text{final}} \in \mathbb{R}^{b \times h}$ is passed through a linear classifier:

$$\mathbf{P} = \mathbf{W}_{\text{cls}} \cdot \mathbf{V}_{\text{final}} + \mathbf{B}, \quad \mathbf{P} \in \mathbb{R}^{b \times 5}$$

where b is the batch size and \mathbf{P} contains the predicted logits over the five veracity labels. We use standard cross-entropy loss to supervise this classification:

$$\mathcal{L}_{\text{CE}} = -\frac{1}{b} \sum_{i=1}^b \log \left(\frac{\exp(Z_{i,y_i})}{\sum_{j=1}^5 \exp(Z_{i,j})} \right)$$

To improve discriminative learning and cross-modal alignment, we have incorporated a symmetric contrastive objective. Projected embeddings of the claim and document representations, denoted as $\mathbf{Z}_{\text{claim}}$ and \mathbf{Z}_{doc} , are normalized:

$$\hat{\mathbf{z}} = \frac{\mathbf{z}}{\|\mathbf{z}\|_2}$$

We then compute the pairwise similarity matrix \mathbf{S} as:

$$\mathbf{S} = \hat{\mathbf{Z}}_{\text{claim}} \cdot \hat{\mathbf{Z}}_{\text{doc}}^\top \in \mathbb{R}^{b \times b}$$

The S_{ij} represents the cosine similarity between the i -th claim and j -th document. Then the InfoNCE loss is computed in both directions:

claim \rightarrow **evidence document**:

$$\text{Loss}_{\text{claim} \rightarrow \text{doc}} = -\frac{1}{b} \sum_{i=1}^b \log \frac{\exp(S_{ii}/\tau)}{\sum_{j=1}^b \exp(S_{ij}/\tau)}$$

document evidence \rightarrow **claim**:

$$\text{Loss}_{\text{doc} \rightarrow \text{claim}} = -\frac{1}{b} \sum_{j=1}^b \log \frac{\exp(S_{jj}/\tau)}{\sum_{i=1}^b \exp(S_{ij}/\tau)}$$

Then the final contrastive loss is the average of both:

$$\mathcal{L}_{\text{contrastive}} = \frac{1}{2} (\text{Loss}_{\text{claim} \rightarrow \text{doc}} + \text{Loss}_{\text{doc} \rightarrow \text{claim}})$$

The total training objective combines classification and contrastive supervision:

$$\mathcal{L}_{\text{total}} = \mathcal{L}_{\text{CE}} + \lambda \cdot \mathcal{L}_{\text{contrastive}}$$

where λ balances the influence of the contrastive signal. We have set $\lambda = 0.1$ in all experiments. This dual-objective training not only improves classification accuracy but also structures the latent space such that semantically aligned claim-document pairs are closer, while unrelated pairs remain well-separated. The contrastive head consistently boosts performance across all evaluated models.

V. EXPERIMENTS:

In this section, we have presented the experiments to evaluate the effectiveness of our framework. We have assessed the impact of different learning strategies, model architectures, and training choices, with a focus on how fusion methods and element-wise operations enhance multimodal relationships.

A. Experimental setup:

All experiments were conducted on a single NVIDIA A100 80GB GPU using PyTorch and Hugging Face Transformers. We evaluated model performance using the weighted F1 score, which balances class-wise F1 scores based on support (i.e., true instance count per class). This metric provides a fairer summary under label imbalance compared to unweighted F1. Formally, if F_i is the F1 score and n_i is the support for class i , then:

$$\text{Weighted-F}_1 = \frac{\sum_i n_i F_i}{\sum_i n_i}$$

We have performed thorough hyperparameter tuning for both the contrastive and non-contrastive variants. The final configuration for the experiments are reported in Table II. We have experimented with a range of pre-trained language models for text and backbone vision encoders for image features. Both modalities are projected into a shared latent space. Code and trained models will be released for reproducibility.

Component	Hyperparameter	Value
Reproducibility	Seeds	42, 57, 196, 906
	Max length	128
Contrastive Loss	Temperature (τ)	0.1
	Loss weight (λ)	0.1
Optimization	Optimizer	Adam
	Learning rate	1×10^{-5}
	Batch size	32
	Num workers	4
	Epochs	20
LR Scheduling	Scheduler	ReduceLROnPlateau
Early Stopping	Patience	5

TABLE II: Hyperparameter settings used in all experiments.

B. Baselines:

For comparative evaluation, we have reproduced the **Pro_CoFactv2** model, originally proposed by [45], which achieves state-of-the-art performance on the Factify 2 benchmark. This model leverages large pretrained encoders: DeBERTa-large for text and SwinV2-base for images along with adapter-based projection layers and a lightweight fusion classifier. Both encoders are unfrozen and trained end-to-end. Pro_CoFactv2 applies linear fusion of text and image features, and jointly optimizes

a multi-loss objective: cross-entropy for classification and a supervised contrastive loss scaled by 0.3 to improve intra-class alignment in the embedding space. We have replicated the original configuration using the same random seeds (42, 57, 196, 906), learning rate (5×10^{-5}), batch size (32), and training duration (20 epochs). Sequence length is set to 128 due to GPU constraints, with a dropout rate of 0.1, 12 attention heads, and an intermediate hidden dimension of 256. Experiments were conducted on a single NVIDIA A100 80GB GPU. Reproduced performance is reported in Table III.

Class	Precision	Recall	F1 Score
Support Text	0.48 (± 0.04)	0.38 (± 0.06)	0.42 (± 0.03)
Support Multimodal	0.50 (± 0.04)	0.61 (± 0.02)	0.55 (± 0.02)
Insufficient Text	0.50 (± 0.01)	0.44 (± 0.07)	0.46 (± 0.04)
Insufficient Multimodal	0.43 (± 0.02)	0.46 (± 0.06)	0.44 (± 0.02)
Refute	0.98 (± 0.00)	0.98 (± 0.00)	0.98 (± 0.00)
Weighted F1 Score	0.57 (± 0.01)		

TABLE III: Performance of the reproduced baseline model (Pro-CoFactv2) on the Factivy 2 dataset.

C. Experimental Variants:

In addition to evaluating the baseline, we conducted experiments to assess the impact of our approach by comparing two main model variants:

With Contrastive Head: This version integrates a contrastive projection head applied to the multimodal representations of claims and evidence documents. Training includes a contrastive loss in addition to the standard cross-entropy loss. This encourages the model to learn modality-consistent and semantically aligned embeddings.

Without Contrastive Head: In this version, the contrastive projection head and the associated loss are omitted. The model relies solely on cross-entropy loss applied to the fused multimodal representation for classification. The only difference is the inclusion of contrastive supervision. Results are presented in Tables IV, V, with discussion in Section VI.

VI. RESULTS AND DISCUSSION:

We evaluated our proposed framework on the Factivy 2 dataset using multiple combinations of language and vision backbones. Performance is measured using weighted F1 scores across five fine-grained veracity labels. We have reported both overall and class-wise results to assess the model’s capabilities. As shown in Tables IV and V, all model variants significantly outperform the baseline. Additionally, models integrated with contrastive head consistently outperform their non-contrastive counterparts. This trend holds across the visual encoders, confirming the robustness of our architecture.

Notably, the marginal gains are observed in “Insufficient” and “Refute” categories that require resolving minor differences between text and images. These results show that our fusion method and contrastive learning help the model to better connect text and images.

A. Insights:

Contrastive learning boosts accuracy: Across all settings, the inclusion of contrastive supervision yields statistically significant gains. It consistently outperforms non-contrastive counterparts, see Table VI. The consistent asymmetry in discordant prediction counts, as shown in Figure 6, confirms that contrastive models correct significantly more baseline errors than they introduce.

Role of fusion strategy: The fusion module using element-wise difference and product provides critical advantages over simple concatenation. These operations help the model clearly match or contrast the claim with the evidence, improving its reasoning.

Model robust nature: Whether paired with ResNet50 or ViT, and regardless of the language encoder, the contrastive head along with fusion module consistently improves performance, highlighting its modularity and general applicability.

VII. ERROR ANALYSIS:

To better understand the behavioral differences between our models and the baseline, we performed a detailed error analysis using both statistical significance tests and qualitative assessments.

Statistical comparisons: we have applied McNemar’s test for overall accuracy and Bowker’s test for class-level shifts. Tables VI, VII show consistently high χ^2 scores with p-values < 0.05 , confirming significant improvements. Whereas Bowker’s results further indicate structured, non-random gains in class predictions.

Discordant pair analysis: We compared our model predictions over the baseline using McNemar’s 2×2 contingency setup to identify disagreement cases. Here, (b) counts instances where the baseline is correct and our model is errors, while (c) captures the opposite. In all five model variants, (c) consistently exceeds (b), as shown in Figure 6, indicating that our model reliably corrects baseline errors. These findings align with significance tests, further validating the effectiveness of our approach. **Qualitative Analysis:** To better understand model behavior, we examined the mismatches between our approach and the baseline. As shown in Figure 5, the baseline overlooked the visual modality entirely and based its decision on text alone, predicting *Insufficient Text*. In contrast, our model incorporated the OCR-detected credit “Helen Sloan/HBO” from the image, identifying it as a licensed promotional photograph a detail suggesting

Models w/ Contrastive Head	Support Text	Support Multimodal	Insufficient Text	Insufficient Multimodal	Refute	Weighted F1 Score
Roberta + ResNet50	0.77 (± 0.02)	0.83 (± 0.01)	0.82 (± 0.00)	0.76 (± 0.02)	1.00 (± 0.00)	0.84 (± 0.01)
Roberta + ViT	0.77 (± 0.02)	0.84 (± 0.01)	0.82 (± 0.00)	0.77 (± 0.01)	1.00 (± 0.00)	0.84 (± 0.01)
DeBERTa + ViT	0.77 (± 0.01)	0.84 (± 0.01)	0.83 (± 0.00)	0.78 (± 0.01)	1.00 (± 0.00)	0.84 (± 0.01)
DeBERTa + ResNet50	0.76 (± 0.02)	0.81 (± 0.02)	0.81 (± 0.01)	0.75 (± 0.02)	1.00 (± 0.00)	0.83 (± 0.01)
SBERT + ResNet50	0.75 (± 0.01)	0.83 (± 0.01)	0.79 (± 0.00)	0.76 (± 0.01)	1.00 (± 0.00)	0.82 (± 0.00)
Baseline	0.42 (± 0.03)	0.55 (± 0.02)	0.46 (± 0.04)	0.44 (± 0.02)	0.98 (± 0.00)	0.57 (± 0.01)

TABLE IV: Class-wise F1 scores and weighted F1 for various model combinations on the Factify 2 dataset with contrastive head. Each value is the mean F1 \pm std across seeds.

Models w/o Contrastive Head	Support Text	Support Multimodal	Insufficient Text	Insufficient Multimodal	Refute	Weighted F1 Score
Roberta + ResNet50	0.74 (± 0.01)	0.82 (± 0.01)	0.78 (± 0.01)	0.75 (± 0.01)	0.99 (± 0.01)	0.82 (± 0.01)
Roberta + ViT	0.75 (± 0.01)	0.82 (± 0.01)	0.79 (± 0.01)	0.75 (± 0.01)	1.00 (± 0.00)	0.82 (± 0.00)
DeBERTa + ViT	0.74 (± 0.01)	0.82 (± 0.00)	0.78 (± 0.01)	0.75 (± 0.01)	1.00 (± 0.00)	0.82 (± 0.00)
DeBERTa + ResNet50	0.74 (± 0.01)	0.81 (± 0.01)	0.78 (± 0.01)	0.74 (± 0.01)	1.00 (± 0.00)	0.81 (± 0.00)
SBERT + ResNet50	0.71 (± 0.03)	0.81 (± 0.02)	0.75 (± 0.02)	0.74 (± 0.02)	0.99 (± 0.00)	0.78 (± 0.05)
Baseline	0.42 (± 0.03)	0.55 (± 0.02)	0.46 (± 0.04)	0.44 (± 0.02)	0.98 (± 0.00)	0.57 (± 0.01)

TABLE V: Class-wise F1 scores and weighted F1 for various model combinations on the Factify 2 dataset (no contrastive head). Each value is mean F1 \pm std across seeds.

Models w/ Contrastive Head	McNemar’s χ^2	McNemar’s p-value	Significance at $\alpha = 0.05$	Bowker’s χ^2 (df=10)	Bowker’s p-value	Reject symmetry
Roberta + ResNet50	1238.56	$\ll 0.05$	✓	91.85	2.33×10^{-15}	✓
Roberta + ViT	1333.14	$\ll 0.05$	✓	132.10	0.00	✓
DeBERTa + ViT	1480.57	$\ll 0.05$	✓	118.33	0.00	✓
DeBERTa + ResNet50	1217.24	$\ll 0.05$	✓	166.16	0.00	✓
SBERT + ResNet50	1070.45	$\ll 0.05$	✓	82.030	2.00×10^{-13}	✓

TABLE VI: Significance-test results comparing the multimodal model against the baseline on Factify 2.

Models w/o Contrastive Head	McNemar’s χ^2	McNemar’s p-value	Significance at $\alpha = 0.05$	Bowker’s χ^2 (df=10)	Bowker’s p-value	Reject symmetry
Roberta + ResNet50	1129.91	$\ll 0.05$	✓	75.64	3.56×10^{-12}	✓
Roberta + ViT	1243.45	$\ll 0.05$	✓	140.44	0.00	✓
DeBERTa + ViT	965.16	$\ll 0.05$	✓	122.93	0.00	✓
DeBERTa + ResNet50	1195.33	$\ll 0.05$	✓	153.76	0.00	✓
SBERT + ResNet50	891.88	$\ll 0.05$	✓	100.06	0.00	✓

TABLE VII: Significance-test results comparing the multimodal model against the baseline on Factify 2.

the image does not contribute new factual content. By recognizing the lack of substantive support in both text and image, our model rightly predicted *Insufficient Multimodal*. This highlights how image provenance, even in OCR form, enhances factual reasoning. Additional examples are discussed below:

Additional examples of qualitative analysis:

We have presented detailed examples mentioned by the original ID of the samples as per the dataset, comparing predictions from our approach against the baseline. These examples illustrate how OCR-based information like photographer credits, agency marks, or image overlays can either resolve or confuse multimodal evidence verifi-

cation.

Example A: When MultiCheck outperforms the baseline

- **ID 4681:** The baseline model, using only textual signals, interpreted the phrase “Made in India vaccines” as concrete evidence supporting the claim thus predicting *Support_Text*. However, the OCR-extracted string “COLO STORAE” (interpreted as “cold storage”) hinted at logistical or infrastructure gaps in the vaccine delivery, casting doubt on the sufficiency of the claim’s evidence. Our model’s multimodal fusion recognized this ambiguity and opted for *Insufficient_Text*, aligning with the ground truth. This example shows how even noisy OCR

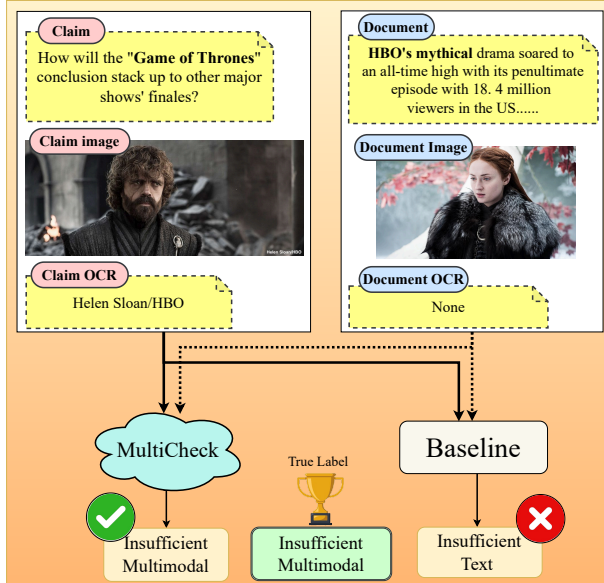


Fig. 5: Example of qualitative analysis, Sample from the dataset.

text can surface hidden context missed by text-only models.

- **ID 6968:** The baseline inferred support based on name and context matches in the text (e.g., “Governor Jagdeep Dhankar”), resulting in a *Support_Text* prediction. However, the image’s OCR output “ANI” indicated it was a generic press photo from a news agency, lacking evidentiary value. Our model correctly interpreted this, combining the weak textual alignment with the non-informative image tag to determine that neither modality offered enough proof thus choosing *Insufficient_Multimodal*. This highlights the model’s ability to ignore superficial visual cues.

Example B: When baseline outperforms MultiCheck

- **ID 7171:** Here, our model was overly cautious. The OCR tag “ANI” led it to interpret the image as a generic stock photo, causing it to discount visual evidence. It then judged the claim as lacking visual proof and labeled it *Insufficient_Multimodal*. However, the textual portion “will lay foundation stone” is a direct and verifiable event announcement, and the image (even if generic) serves as a credible contextual anchor. The baseline, focusing on the assertive language in the text, correctly predicted *Support_Multimodal*. This example shows that OCR can occasionally mislead, especially when image content is generic but still contextually supportive.

Key Observations:

- **OCR text can be highly informative** especially when images include meta-tags, banners, or visual

overlays not present in article text.

- **Failure cases arise** when OCR includes irrelevant or misleading tokens, causing the model to over- or under-attend to visuals.
- **Future directions:** We plan to incorporate an OCR quality gating mechanism and synthetic noisy-OCR augmentation to improve model robustness.

VIII. CONCLUSION:

This paper introduces a unified framework for fine-grained multimodal fact-checking that jointly reasons over textual and visual evidence. Our architecture integrates structured representations from pre-trained language and vision models using a relational fusion module. It further employs a contrastive learning objective to enhance cross-modal alignment. This design allows the model to better capture fine agreements and contradictions between claims and evidence across modalities. As our approach outperforms the baseline, across multiple configurations. It achieves particularly notable gains in complex classes such as “*Insufficient*” and “*Refute*”, where multimodal reasoning is critical. Statistical tests and qualitative analyses confirm that the improvements are consistent and meaningful. These gains are systematic, rather than incidental. Overall, our results emphasize the importance of explicit cross-modal alignment and representation learning in advancing automated fact verification.

IX. LIMITATION:

While our approach shows strong empirical performance, several limitations remain:

- **Dependence on OCR quality:** The model incorporates OCR-extracted text from images, which can vary widely in accuracy and relevance. In cases of noisy or misleading OCR outputs, the model may misclassify due to spurious visual-textual alignment.
- **No evidence retrieval component:** Our framework assumes that relevant evidence both textual and visual is already provided. It does not include any retrieval pipeline to source additional or more reliable evidences from external knowledge bases or web sources.
- **Limited visual understanding:** Although image features are included via pre-trained encoders, the model lacks deeper visual reasoning capabilities such as object detection, scene understanding, or temporal cues that could improve evidence grounding.
- **Restricted modalities:** The current system handles only text and image modalities. It does not address audio, video, or temporal multimodal misinformation, which are common in modern social media content.

REFERENCES

- [1] M. M. F. Caceres, J. P. Sosa, J. A. Lawrence, C. Sestacovschi, A. Tidd-Johnson, M. H. U. Rasool, V. K. Gadamidi, S. Ozair, K. Pandav, C. Cuevas-Lou *et al.*, “The impact of misinformation on the covid-19 pandemic,” *AIMS public health*, vol. 9, no. 2, p. 262, 2022.
- [2] G. Murphy, C. de Saint Laurent, M. Reynolds, O. Aftab, K. Hegarty, Y. Sun, and C. M. Greene, “What do we study when we study misinformation? a scoping review of experimental research (2016-2022),” *Harvard Kennedy School Misinformation Review*, 2023.
- [3] B. Kim, A. Xiong, D. Lee, and K. Han, “A systematic review on fake news research through the lens of news creation and consumption: Research efforts, challenges, and future directions,” *PLoS one*, vol. 16, no. 12, p. e0260080, 2021.
- [4] G. Di Domenico, J. Sit, A. Ishizaka, and D. Nunan, “Fake news, social media and marketing: A systematic review,” *Journal of business research*, vol. 124, pp. 329–341, 2021.
- [5] S. Abdali, S. Shaham, and B. Krishnamachari, “Multi-modal misinformation detection: Approaches, challenges and opportunities,” *ACM Computing Surveys*, vol. 57, no. 3, pp. 1–29, 2024.
- [6] D. A. Mura, M. Usai, A. Loddo, M. Sanguinetti, L. Zedda, C. Di Ruberto, and M. Atzori, “Is it fake or not? a comprehensive approach for multimodal fake news detection,” *Online Social Networks and Media*, vol. 47, p. 100314, 2025.
- [7] J. Askari, “Deepfakes and synthetic media: What are they and how are tech members taking steps to tackle misinformation and fraud,” *TechUK*, vol. 18, 2023.
- [8] S. Tufchi, A. Yadav, and T. Ahmed, “A comprehensive survey of multimodal fake news detection techniques: advances, challenges, and opportunities,” *International Journal of Multimedia Information Retrieval*, vol. 12, no. 2, p. 28, 2023.
- [9] T. Braun, M. Rothermel, M. Rohrbach, and A. Rohrbach, “Defame: Dynamic evidence-based fact-checking with multimodal experts,” *arXiv preprint arXiv:2412.10510*, 2024.
- [10] M. Akhtar, M. Schlichtkrull, Z. Guo, O. Cocarascu, E. Simperl, and A. Vlachos, “Multimodal automated fact-checking: A survey,” in *Findings of the Association for Computational Linguistics: EMNLP 2023*, 2023, pp. 5430–5448.
- [11] J. Thorne, A. Vlachos, C. Christodoulopoulos, and A. Mittal, “FEVER: a large-scale dataset for fact extraction and VERification,” in *Proceedings of the 2018 Conference of the North American Chapter of the Association for Computational Linguistics: Human Language Technologies, Volume 1 (Long Papers)*, M. Walker, H. Ji, and A. Stent, Eds. New Orleans, Louisiana: Association for Computational Linguistics, Jun. 2018, pp. 809–819. [Online]. Available: <https://aclanthology.org/N18-1074/>
- [12] Y. Yao, Y. Du, C. Wang, and K. Shu, “Mocheg: Multimodal contrastive hybrid evidence generation for multimodal fact-checking,” in *Findings of the Association for Computational Linguistics: ACL 2023*, 2023, pp. 10433–10447.
- [13] S. Suryavardan, S. Deshpande, L. Li, T. Dadu, P. Kalluri, S. Shaar, L. Zhang, and P. Nakov, “Factify 2: Towards fine-grained multimodal fact verification with social media evidence,” in *Findings of the Association for Computational Linguistics: EMNLP 2023*, 2023.
- [14] Y.-C. Chen, L. Li, L. Yu, A. El Kholly, F. Ahmed, Z. Gan, Y. Cheng, and J. Liu, “Uniter: Universal image-text representation learning,” in *European conference on computer vision*. Springer, 2020, pp. 104–120.
- [15] J. Lu, D. Batra, D. Parikh, and S. Lee, “Vilbert: Pretraining task-agnostic visiolinguistic representations for vision-and-language tasks,” in *Advances in Neural Information Processing Systems (NeurIPS)*, 2019.
- [16] Y. Du, Y. Yao, C. Wang, and K. Shu, “Precofactv2: Improving multimodal fact-checking via precise and coarse-grained evidence matching,” in *Findings of the Association for Computational Linguistics: ACL 2023*, 2023, pp. 14671–14685.
- [17] W.-W. Du, H.-W. Wu, W.-Y. Wang, and W.-C. Peng, “Team triple-check at factify 2: Parameter-efficient large foundation models with feature representations for multi-modal fact verification,” in *DE-FACTIFY@ AAAI*, 2023.
- [18] A. Conneau, D. Kiela, H. Schwenk, L. Barrault, and A. Bordes, “Supervised learning of universal sentence representations from natural language inference data,” in *Proceedings of the 2017 Conference on Empirical Methods in Natural Language Processing*, 2017, pp. 670–680.
- [19] J.-H. Kim, J. Jun, and B.-T. Zhang, “Bilinear attention networks,” *Advances in neural information processing systems*, vol. 31, 2018.
- [20] A. v. d. Oord, Y. Li, and O. Vinyals, “Representation learning with contrastive predictive coding,” *arXiv preprint arXiv:1807.03748*, 2018.
- [21] R. F. Cekinel, P. Karagoz, and Ç. Çöltekin, “Multimodal fact-checking with vision language models: A probing classifier based solution with embedding strategies,” in *Proceedings of the 31st International Conference on Computational Linguistics*, 2025, pp. 4622–4633.
- [22] S. Abdelnabi, R. Hasan, and M. Fritz, “Open-domain, content-based, multi-modal fact-checking of out-of-context images via online resources,” in *Proceedings of the IEEE/CVF conference on computer vision and pattern recognition*, 2022, pp. 14940–14949.
- [23] J. Thorne, A. Vlachos, C. Christodoulopoulos, and A. Mittal, “Fever: a large-scale dataset for fact extraction and verification,” in *Proceedings of the 2018 Conference of the North American Chapter of the Association for Computational Linguistics: Human Language Technologies, Volume 1 (Long Papers)*, 2018, pp. 809–819.
- [24] P. Nakov, D. Corney, M. Hasanain, F. Alam, T. Elsayed, A. Barrón-Cedeño, P. Papotti, S. Shaar, and G. da San Martino, “Automated fact-checking for assisting human fact-checkers,” in *30th International Joint Conference on Artificial Intelligence, IJCAI 2021*. International Joint Conferences on Artificial Intelligence, 2021, pp. 4551–4558.
- [25] M. Hameleers, T. E. Powell, T. G. Van Der Meer, and L. Bos, “A picture paints a thousand lies? the effects and mechanisms of multimodal disinformation and rebuttals disseminated via social media,” *Political Communication*, vol. 37, no. 2, pp. 281–301, 2020.
- [26] F. Alam, S. Cresci, T. Chakraborty, F. Silvestri, D. Dimitrov, G. Da San Martino, S. Shaar, H. Firooz, and P. Nakov, “A survey on multimodal disinformation detection,” in *Proceedings of the 29th International Conference on Computational Linguistics*, 2022, pp. 6625–6643.
- [27] D. Zlatkova, P. Nakov, and I. Koychev, “Fact-checking meets fauxtography: Verifying claims about images,” in *Proceedings of the 2019 Conference on Empirical Methods in Natural Language Processing and the 9th International Joint Conference on Natural Language Processing (EMNLP-IJCNLP)*, K. Inui, J. Jiang, V. Ng, and X. Wan, Eds. Hong Kong, China: Association for Computational Linguistics, Nov. 2019, pp. 2099–2108. [Online]. Available: <https://aclanthology.org/D19-1216/>
- [28] M. A. Khaliq, P. Y.-C. Chang, M. Ma, B. Pflugfelder, and F. Miletic, “RAGAR, your falsehood radar: RAG-augmented reasoning for political fact-checking using multimodal large language models,” in *Proceedings of the Seventh Fact Extraction and VERification Workshop (FEVER)*, M. Schlichtkrull, Y. Chen, C. Whitehouse, Z. Deng, M. Akhtar, R. Aly, Z. Guo, C. Christodoulopoulos, O. Cocarascu, A. Mittal, J. Thorne, and A. Vlachos, Eds. Miami, Florida, USA: Association for Computational Linguistics, Nov. 2024, pp. 280–296. [Online]. Available: <https://aclanthology.org/2024.fever-1.29/>
- [29] R. F. Cekinel, P. Karagoz, and Ç. Çöltekin, “Multimodal fact-checking with vision language models: A probing classifier based solution with embedding strategies,” in *Proceedings of the 31st International Conference on Computational Linguistics*, O. Rambow, L. Wanner, M. Apidianaki, H. Al-Khalifa, B. D. Eugenio, and S. Schockaert, Eds. Abu Dhabi, UAE: Association for Computational Linguistics, Jan. 2025, pp. 4622–4633. [Online]. Available: <https://aclanthology.org/2025.coling-main.310/>
- [30] W. W. Du, H. W. Wu, W. Y. Wang, and W. C. Peng, “Team triple-check at factify 2: Parameter-efficient large foundation models

- with feature representations for multi-modal fact verification,” in *CEUR Workshop Proceedings*, vol. 3555. CEUR-WS, 2024.
- [31] Z. Jin, J. Cao, H. Guo, Y. Zhang, and J. Luo, “Multimodal fusion with recurrent neural networks for rumor detection on microblogs,” in *Proceedings of the 25th ACM international conference on Multimedia*, 2017, pp. 795–816.
- [32] K. Shu, D. Mahudeswaran, S. Wang, D. Lee, and H. Liu, “Fakenewsnet: A data repository with news content, social context, and spatiotemporal information for studying fake news on social media,” *Big data*, vol. 8, no. 3, pp. 171–188, 2020.
- [33] B. M. Yao, A. Shah, L. Sun, J.-H. Cho, and L. Huang, “End-to-end multimodal fact-checking and explanation generation: A challenging dataset and models,” in *Proceedings of the 46th International ACM SIGIR Conference on Research and Development in Information Retrieval*, 2023, pp. 2733–2743.
- [34] Y. Liu, M. Ott, N. Goyal, J. Du, M. Joshi, D. Chen, O. Levy, M. Lewis, L. Zettlemoyer, and V. Stoyanov, “Roberta: A robustly optimized bert pretraining approach,” *arXiv preprint arXiv:1907.11692*, 2019.
- [35] P. He, X. Liu, J. Gao, and W. Chen, “Deberta: Decoding-enhanced bert with disentangled attention,” *arXiv preprint arXiv:2006.03654*, 2020.
- [36] N. Reimers and I. Gurevych, “Sentence-bert: Sentence embeddings using siamese bert-networks,” in *Proceedings of the 2019 Conference on Empirical Methods in Natural Language Processing and the 9th International Joint Conference on Natural Language Processing (EMNLP-IJCNLP)*, 2019, pp. 3982–3992.
- [37] K. He, X. Zhang, S. Ren, and J. Sun, “Deep residual learning for image recognition,” in *Proceedings of the IEEE conference on computer vision and pattern recognition*, 2016, pp. 770–778.
- [38] A. Dosovitskiy, L. Beyer, A. Kolesnikov, D. Weissenborn, X. Zhai, T. Unterthiner, M. Dehghani, M. Minderer, G. Heigold, S. Gelly *et al.*, “An image is worth 16x16 words: Transformers for image recognition at scale,” in *International Conference on Learning Representations*, 2020.
- [39] R. Mishra, D. Gupta, and M. Leippold, “Generating fact checking summaries for web claims,” in *EMNLP W-NUT 2020: Conference on Empirical Methods in Natural Language Processing (EMNLP)*, 2020.
- [40] I. Sata, M. Amagasaki, and M. Kiyama, “Multimodal retrieval method for images and diagnostic reports using cross-attention,” *AI*, vol. 6, no. 2, p. 38, 2025.
- [41] X. Wang, M. Gui, Y. Jiang, Z. Jia, N. Bach, T. Wang, Z. Huang, and K. Tu, “Ita: Image-text alignments for multi-modal named entity recognition,” in *Proceedings of the 2022 Conference of the North American Chapter of the Association for Computational Linguistics: Human Language Technologies*, 2022, pp. 3176–3189.
- [42] Y. Liu, G. Li, and L. Lin, “Cross-modal causal relational reasoning for event-level visual question answering,” *IEEE Transactions on Pattern Analysis and Machine Intelligence*, vol. 45, no. 10, pp. 11 624–11 641, 2023.
- [43] H. Gong, W. Xu, S. Wu, Q. Liu, and L. Wang, “Heterogeneous graph reasoning for fact checking over texts and tables,” in *Proceedings of the Thirty-Eighth AAAI Conference on Artificial Intelligence and Thirty-Sixth Conference on Innovative Applications of Artificial Intelligence and Fourteenth Symposium on Educational Advances in Artificial Intelligence*, 2024, pp. 100–108.
- [44] D. Hendrycks and K. Gimpel, “Gaussian error linear units (gelus),” *arXiv preprint arXiv:1606.08415*, 2016.
- [45] W. W. Du, H. W. Wu, W. Y. Wang, and W. C. Peng, “Team triple-check at factify 2: Parameter-efficient large foundation models with feature representations for multi-modal fact verification,” in *CEUR Workshop Proceedings*, vol. 3555. CEUR-WS, 2024.



Fig. 6: Comparison of discordant-pair barplots (first column per model) and McNemar 2×2 contingency heatmaps (second column per model), both with and without the contrastive head. Models (top to bottom): Roberta + ResNet50, Roberta + ViT, DeBERTa + ViT, DeBERTa + ResNet50, SBERT + ResNet50.